SLIDING MODE CONTROL OF INTERLEAVED DOUBLE DUAL BOOST CONVERTER FOR ELECTRIC VEHICLES AND RENEWABLE ENERGY CONVERSION

J. S. V. Siva Kumar[1,2] and P. Mallikarjuna Rao[1]

[1]Department of Electrical Engineering
Andhra University
Visakhapatnam-530003, Andhra Pradesh, India
jsvsivakumar99@gmail.com

[2]Department of Electrical and Electronics Engineering
GMR Institute of Technology (GMRIT)
GMR Nagar, Rajam-532127, Srikakulam District, Andhra Pradesh, India
sivakumar.jsv@gmrit.edu.in

ABSTRACT. *With carbon-negativity as a theme, automobile industry has shifted focus towards green technology, electric vehicles. The push towards electric vehicles is estimated to boost air quality in urban areas where vehicle density is more, hence greenhouse gas emissions are rampant. Of the available green technologies, fuel cell provides higher energy density although at an expense of price. In view of this, a proper mechanism has to be derived to utilize the energy efficiently to make the electric vehicles affordable. Owing to the low voltage output from fuel cell, boost converters are used to meet the load requirements. Non-isolated Interleaved Double Dual Boost (IDDB) converters are recommended to augment the efficiency of the converter and in turn to reduce overall weight of the vehicle. In this paper, sliding mode control technique is implemented to improve the transient response of the fuel cell powered IDDB converter for various load conditions. The results are verified in the simulated environment using MATLAB/Simulink.*
Keywords: Electric vehicle, Non-isolated boost converter, Interleaved double dual boost converter, High voltage gain, Sliding mode control

1. **Introduction.** Transportation plays a key role in the development of an economy. However, due to the usage of fossil fuels, carbon-based compounds, in the current vehicles, result in enormous amounts of greenhouse gases. According to several studies, most of the densely populated cities are facing detrimental air quality. In contrast, electric vehicles use electrical energy for propulsion, resulting in eco-friendly transportation. Electric vehicles use battery, ultra-capacitor, Fuel Cell (FC) as energy source for propulsion system. Of these, fuel cell, due to high power density and green source of electrical energy, was proved to be a better choice as a primary source of energy in EV. However, due to the slower response of FC, they cannot respond faster for sudden changes in load and hence an ultra-capacitor is recommended for propulsion system during dynamic condition. Ultra-capacitors have high energy density but low power densities, which make them charge as well as discharge at a faster rate. This nature allows the ultra-capacitor to provide the energy during transients [1].

Normally voltage level of FC is very low and the drive motor for which FC supply energy operates at high voltage level. Hence, a step-up power chopper is required to boost the voltage level of FC. It is quite a challenging task to maintain high efficiency at such voltage gain requirements [2-5]. For a given power, low input voltage results in high input current. For such a high current, the boost converter has to be operated at small

duty cycle which forces the size of inductor and output capacitor to the upside [1], and increases losses, resulting in less efficient converter [10].

Hence, for high power application such as EV a high power converter is required for boosting up voltage level of FC, which can deal with high current and high voltage at the input and output respectively without affecting efficiency [6]. Most efficient way to tackle this problem is by interleaving multiple conventional-boost converters.

This paper verifies the viability of interleaved double dual boost proposed with the objective of achieving higher voltage gain in contrast to the classical boost converter [1-5]. This topology was chosen among others that also have high gain properties [6-8] owing to the possibility of phase interleaving that allows the modular characteristics of the converter for high power applications.

An efficient controller is required for regulating output voltage at the nominal value even under load perturbations that typically happen in electric vehicles [9]. This paper presents a sliding mode control of an interleaved double dual boost converter and its effectiveness is verified under various load disturbances in a simulation environment, MATLAB/Simulink.

2. **Modeling of the N-Phase IDDB Converter.** The IDDB with two phases is shown in Figure 1, where 'R_0' represents the load. Each phase of the converter comprises a conventional boost module with an inductor and its corresponding pair of switches. Phase 1 and capacitor C_1 are here denoted by "module-1" vice versa.
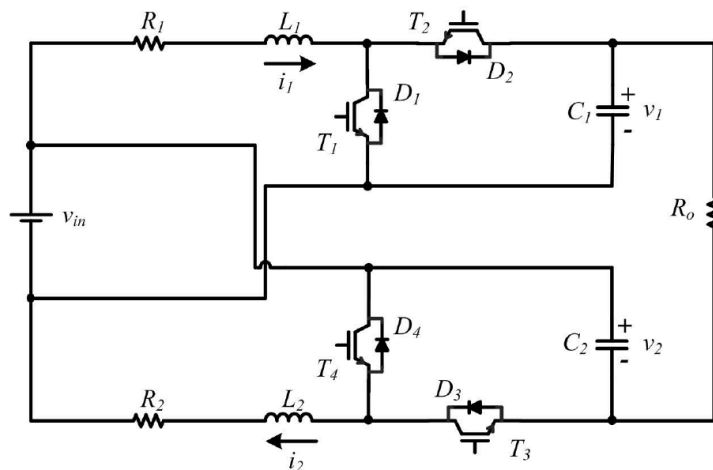
FIGURE 1. IDDB with two phases

Assumption: Two modules of the converter are symmetric.

The variable δ is the duty cycle and it is identical to both the modules. The model is concerned with the capacitors voltages that have an indirect relationship with output voltage. However, it is noteworthy that the output voltage indirectly depends on the input voltage. This infers that any change in input voltage reflects in the output voltage and can be compensated by regulating output-capacitor voltage references. Any attempt to directly control the output voltage, ignoring module voltages, would result in an imbalance of these voltages, resulting in distorted symmetry in the wave shape.

As pointed, this topology facilitates modular structure permitting more than two phases. In order to attain symmetry, an even multiple of phases are preferred. This section is to generalise the converter modelling to N-phase topology.

The combination of the phases that are connected to the capacitor C_1 and capacitor C_2 itself forms module-1 and vice versa for module-2. As a demonstration, the six-phase converter is shown in Figure 2 to depict multiple phases.

The source current is given by:

$$i_{in} = i_1 + i_2 + i_3 + \cdots + i_N - i_0 \tag{1}$$
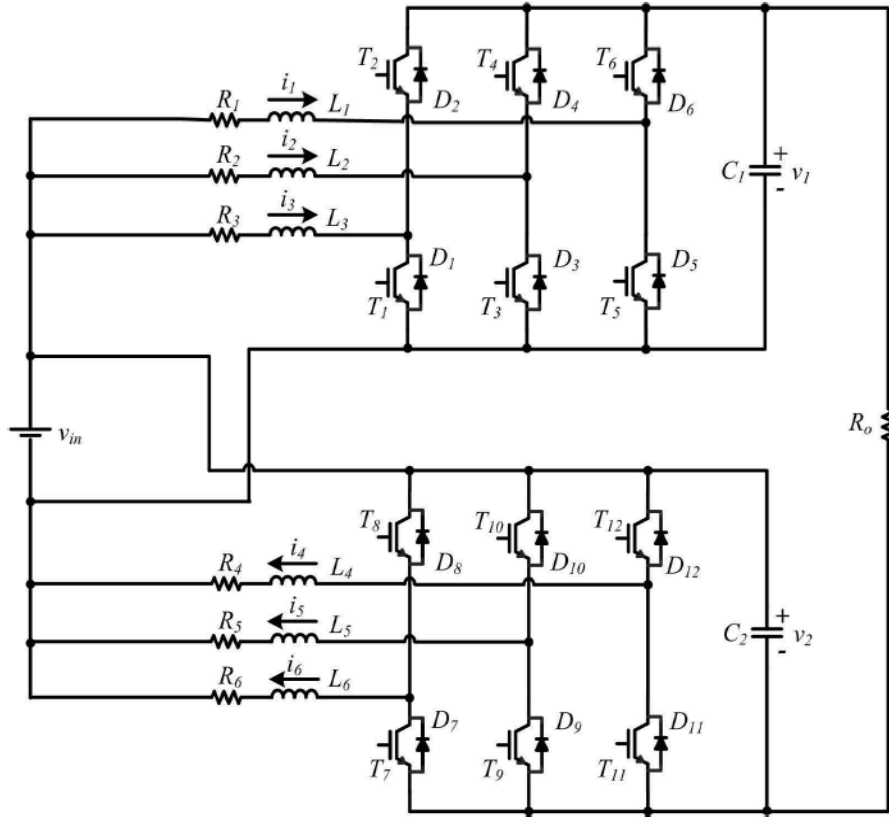
FIGURE 2. Six phase IDDB converter

The N-phase IDDB has $N + 2$ state variables, here chosen as the representing 'N' inductor currents and two capacitor voltages.

The differential equation for the current in each of the $N/2$ inductors of module-1 is given by

$$\frac{d}{dt}I_k = \frac{1}{L_k}\left(-R_k I_k - V_1\bar{\delta}_k + V_{in}\right) \tag{2}$$

for $k = 1, \ldots, N/2$. It is similar for $k = (N/2) + 1$ to N.

The differential equation for the voltage in C_1 is given by V_1

$$\frac{d}{dt}V_1 = \frac{1}{C_1}\left[\left(\sum_{k=1}^{\frac{N}{2}} I_k\bar{\delta}_k\right) + \frac{-V_1 - V_2 + V_{in}}{R_0}\right] \tag{3}$$

It is similar for voltage across C_2.

Now, by exploring the symmetry of the system same like two phase all inductances and capactors are same and also, using the same current reference for the currents of each module, the current in every phase is the same, i.e., $I_1 = I_2 = \cdots = I_N = I$ and the duty cycle is the same for all phases, i.e., $\delta_1 = \delta_2 = \cdots = \delta_N = \delta$.

Then

$$\frac{d}{dt}I = \frac{1}{L}\left(-RI - V\bar{\delta} + V_{in}\right) \tag{4}$$

and

$$\frac{d}{dt}V = \frac{1}{C}\left[\frac{(N\bar{\delta}I)}{2} + \frac{-2V + V_{in}}{R_0}\right] \tag{5}$$

In the state-space form, the state vector is

$$X = \begin{bmatrix} I & V \end{bmatrix}^I \tag{6}$$

while the system and input matrix are

$$A = \begin{bmatrix} \dfrac{-R}{L} & \dfrac{-\bar{\delta}}{L} \\ \dfrac{N\bar{\delta}}{2C} & \dfrac{-2}{R_0C} \end{bmatrix} \quad B = \begin{bmatrix} \dfrac{1}{L} \\ \dfrac{1}{R_0C} \end{bmatrix} \tag{7}$$

The set of attainable equilibrium points of the converter is given by

$$X_{eq} = -A^{-1}BU. \tag{8}$$

Using above, the set of equilibrium points can be written as

$$X_{eq} = \begin{bmatrix} I_{eq} \\ V_{eq} \end{bmatrix} = \begin{bmatrix} \dfrac{2+2\delta}{4R + NR_0\left(1-\delta\right)^2} \\ \dfrac{2R + NR_0\left(1-\delta\right)}{4R + NR_0\left(1-\delta\right)^2} \end{bmatrix} \tag{9}$$

Using the state-space averaging method [2,4,5] and assuming the small-signal approximation, the equivalent linear system near the equilibrium point is given by

$$\dot{\tilde{x}} = A\tilde{x} + [(A_1 - A_2)X + (B_1 - B_2)U]\tilde{\delta} \tag{10}$$

where A_1 and A_2 are the matrices when δ value for 1 and 0 respectively. X means the value of X at equilibrium point.

Using above values the equation can be simplified into

$$\dot{\tilde{x}} = A\tilde{x} + [(A_1 - A_2)X]\tilde{\delta} \tag{11}$$

Substituting all the above values, finally we get

$$\dot{\tilde{x}} = \begin{bmatrix} \dot{\tilde{i}} \\ \dot{\tilde{v}} \end{bmatrix} = \begin{bmatrix} \dfrac{-R}{L}\tilde{i} - \dfrac{\bar{\delta}}{L}\tilde{v} + \dfrac{V_{in}}{L}\left\{ \dfrac{2R + NR_0(1-\delta)}{4R + NR_0(1-\delta)^2} \right\}\tilde{\delta} \\ \dfrac{N\bar{\delta}}{2C}\tilde{i} - \dfrac{2}{R_0C}\tilde{v} - \dfrac{NV_{in}}{2C}\left\{ \dfrac{(2+2\delta)}{4R + NR_0(1-\delta)^2} \right\}\tilde{\delta} \end{bmatrix} \tag{12}$$

3. **Methodology of Sliding Mode Controller.** With reference currents of the inductors are generated using small signal analysis, a feedback controller should be designed to guide the currents towards the reference. Due to fast and robustness requirement of the converter performance, a sliding mode controller is designed, which is a large signal model resulting in global stability. A sliding surface is defined as

$$S = \tilde{v} + k\tilde{i}$$
$$\dot{S} = \dot{\tilde{v}} + k\dot{\tilde{i}}$$

$$\dot{S} = \dfrac{N\tilde{\delta}}{2C}\tilde{i} - \dfrac{2}{R_0C}\tilde{v} - \dfrac{NV_{in}}{2C}\left\{ \dfrac{(2+2\delta)}{4R + NR_0(1-\delta)^2} \right\}\tilde{\delta}$$
$$+ k\left[\dfrac{-R}{L}\tilde{i} - \dfrac{\bar{\delta}}{L}\tilde{v} + \dfrac{V_{in}}{L}\left\{ \dfrac{2R + NR_0(1-\delta)}{4R + NR_0(1-\delta)^2} \right\} \right]\tilde{\delta} \tag{13}$$

Separating $\tilde{v}$, $\tilde{i}$ terms and $\tilde{\delta}$ terms, then we get

$$\dot{S} = \dfrac{N\tilde{\delta}}{2C}\tilde{i} - \dfrac{2}{R_0C}\tilde{v} - k\dfrac{R}{L}\tilde{i} - k\dfrac{\bar{\delta}}{L}\tilde{v}$$
$$+ \left[k\dfrac{V_{in}}{L}\left\{ \dfrac{2R + NR_0(1-\delta)}{4R + NR_0(1-\delta)^2} \right\} - \dfrac{NV_{in}}{2C}\left\{ \dfrac{(2+2\delta)}{4R + NR_0(1-\delta)^2} \right\} \right]\tilde{\delta} \tag{14}$$

Sliding mode will be there when $\dot{S} = 0$.

The generalized control structure

$$u = -f(x) - k_1 sign(S) \qquad (15)$$

From the above equation controlling signal $\tilde{\delta}$ is obtained

$$\tilde{\delta} = \frac{\left[\left\{-\frac{N\bar{\delta}}{2C}\tilde{i} + \frac{2}{R_0 C}\tilde{v} + k\frac{R}{L}\tilde{i} + k\frac{\bar{\delta}}{L}\tilde{v}\right\} - k_1 sign(s)\right]}{\left[k\frac{V_{in}}{L}\left\{\frac{2R+NR_0(1-\delta)}{4R+NR_0(1-\delta)^2}\right\} - \frac{NV_{in}}{2C}\left\{\frac{(2+2\delta)}{4R+NR_0(1-\delta)^2}\right\}\right]} \qquad (16)$$

The control diagram of implemented controller is shown in Figure 3. V_1 and V_2 are the module-1 and module-2 capacitor-voltages respectively. i_1, i_2, i_3, i_4, i_5 and i_6 are respective phase currents. V_1 is the DC link voltage input to the sliding mode controller for module-1 while V_2 is for the module-2. Similarly, i_1, i_2 and i_3 are the input to sliding mode controller of module-1 and i_4, i_5 and i_6 are the input to the module-2 sliding mode controller. Duty ratio is the output of the SMC and is used to generate PWM pulses to control the power switches.
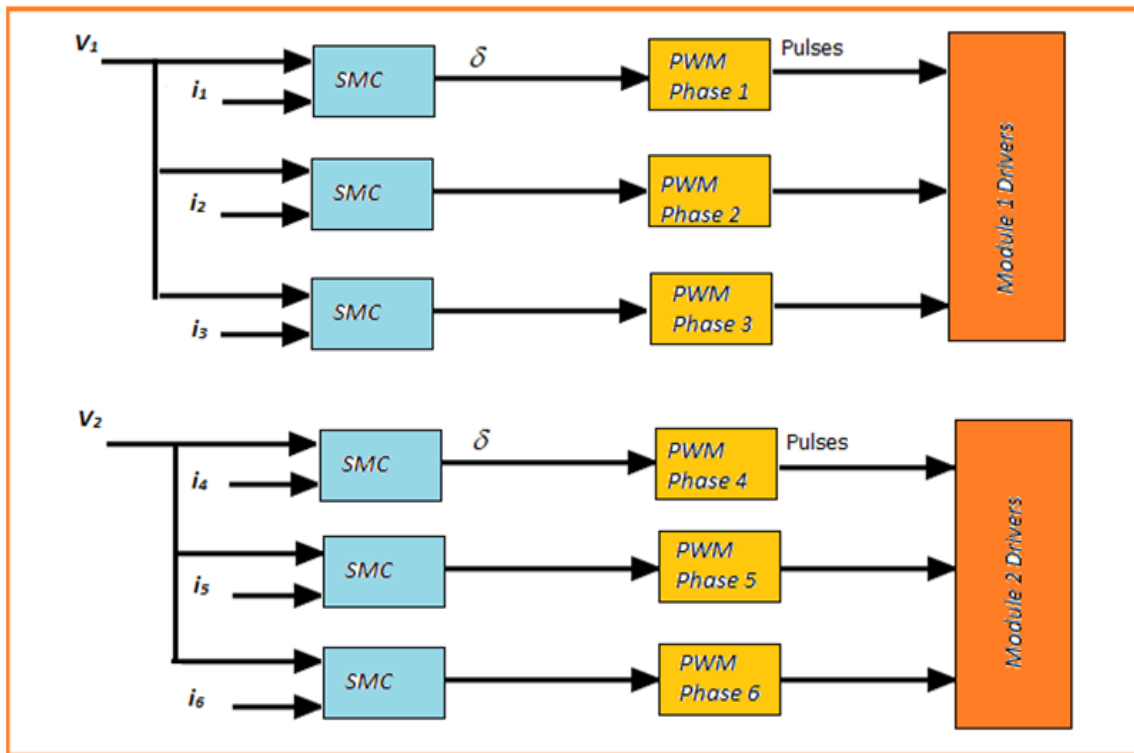
FIGURE 3. Control diagram of the implemented controllers

4. **Results and Discusions.** The IDDB converter is modelled and its performance of the system by employing sliding mode controller is verified on MATLab/Simulink. The results of whole system parameters are shown below. In these two phases and six phase IDDB converter with sliding mode controller simulation results are explained.

The PWM pulses that are fed to two first-phase IGBTs are depicted in Figure 4. From the above it is clear that both switches are operating simultaneously.

The current flowing through the inductance of the two phases is presented in Figure 5. It is clearly observed that the current in each inductance has a current ripple of 8 A. So that the size of inductance L_1 and L_2 can be reduced as well as power handling capacity of the conventional boost converter is increased by using IDDB converter.

Output current is shown Figure 6. In this it is observed the output current value is maintained constant. From Figure 7 the sliding surface also came to constant.

TABLE 1. Parameter values

Parameter	Description	Value
V_{in}	Input Voltage	60 V
R	Series Resistance	0.15 Ω
L	Inductance	535 μH
C	Capacitance	470 μF
R_0	Load Resistance	59 Ω
f_{sw}	Switching Frequency	10 kHz
δ	Duty Cycle	0.73
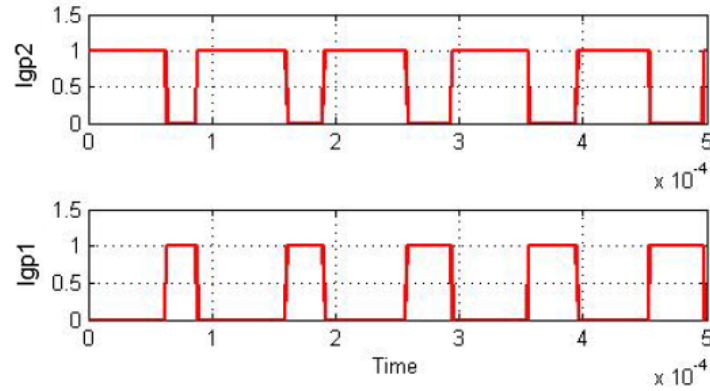
FIGURE 4. PWM pulses to IGBTs
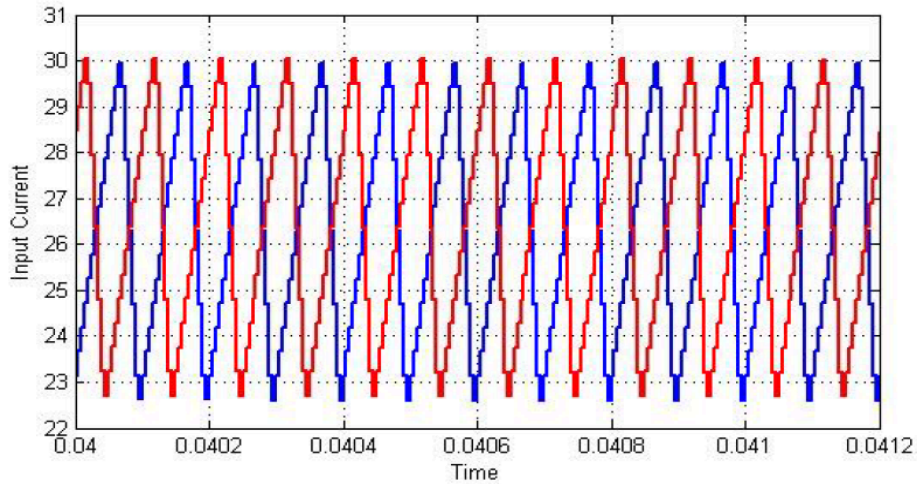
FIGURE 5. (color online) Input current to two phase IDDB

The output voltages, voltage across the capacitors in both phases are shown in Figure 8. From the above the output voltage is regulated at the reference point and capacitor voltages are also constant from the given 60 V input by using sliding mode controller. It is clear from Figure 8 that the fuel cell voltage, 60 V, is boosted to 380 V with the help of IDDB converter and maintaining constant 380 V at load side using sliding mode controller.

The dynamic performance of the sliding mode controller is also evaluated. Figure 9 shows its effectiveness for a step load change from 3 kW to 4 kW, the input voltage regulated by SM controller can come back to the nominal value after a regulating period by regulating the output voltage to the desired value in a short time. However, in practice, parameter variations may creep into the components. In order to demonstrate the validity
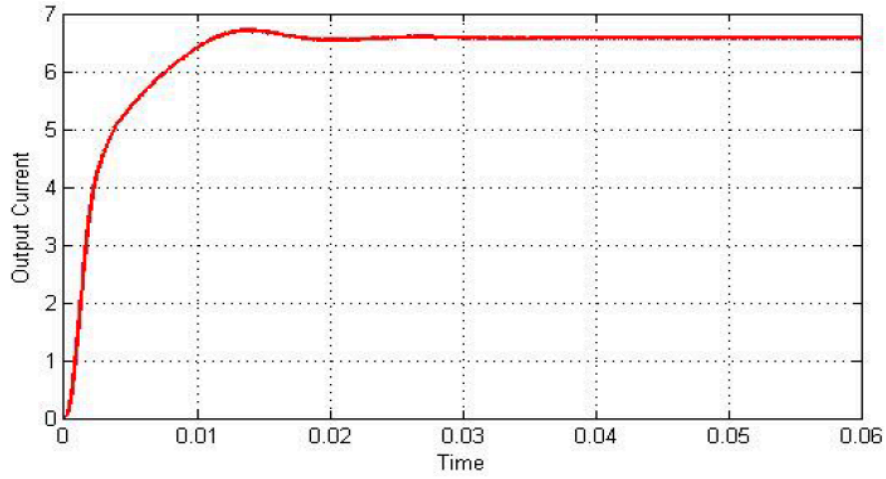
FIGURE 6. Output current of two phase IDDB
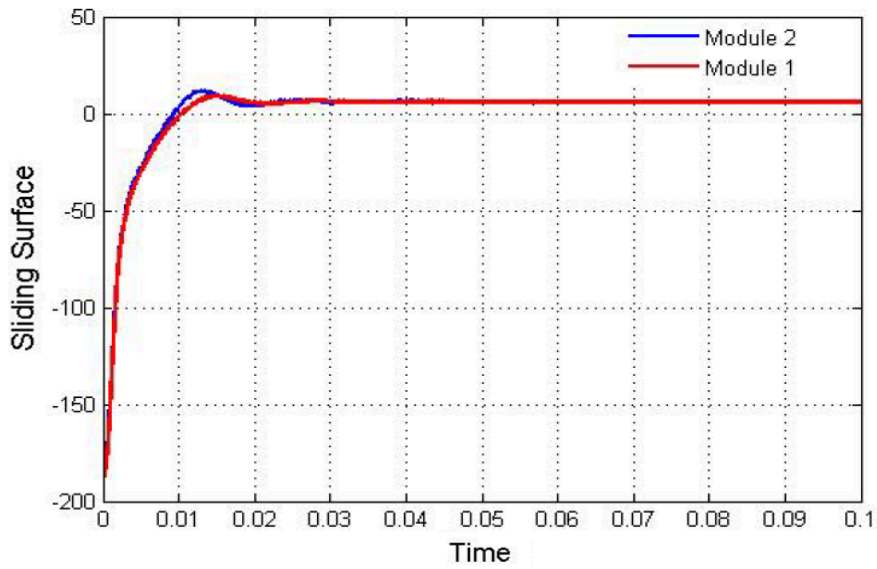
FIGURE 7. (color online) Sliding surface of two phase IDDB
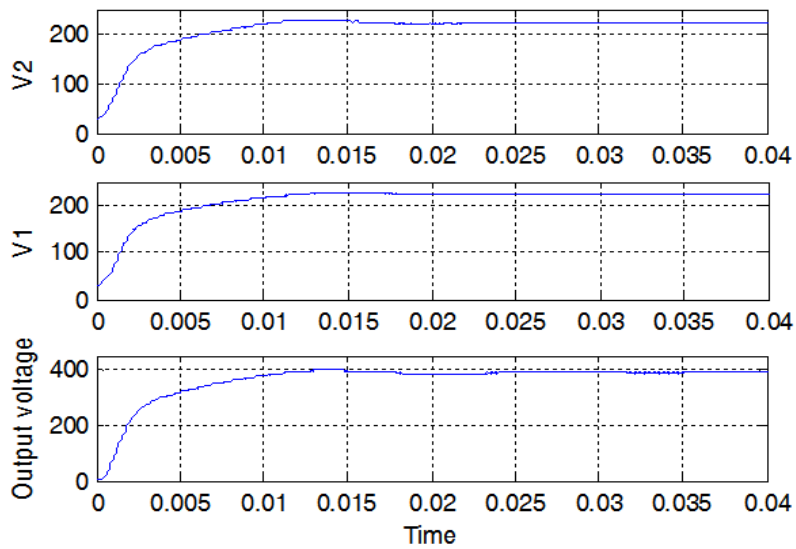
FIGURE 8. Output voltage of two phase IDDB
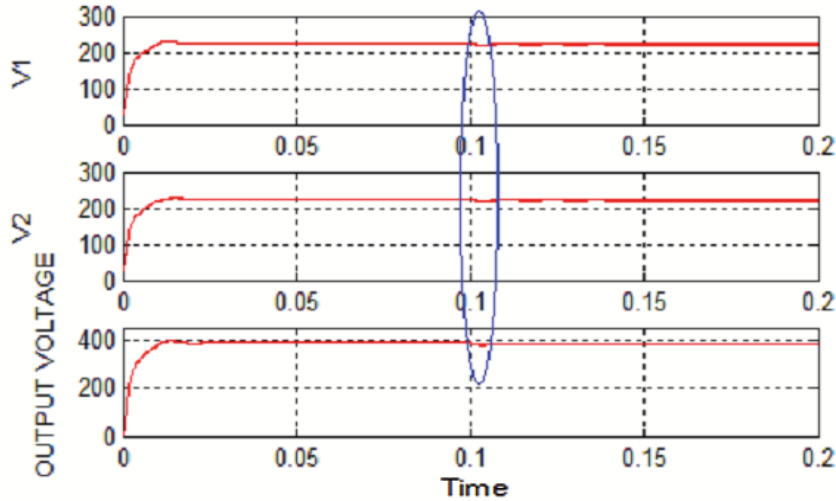
FIGURE 9. Waveforms of the converter in dynamic state
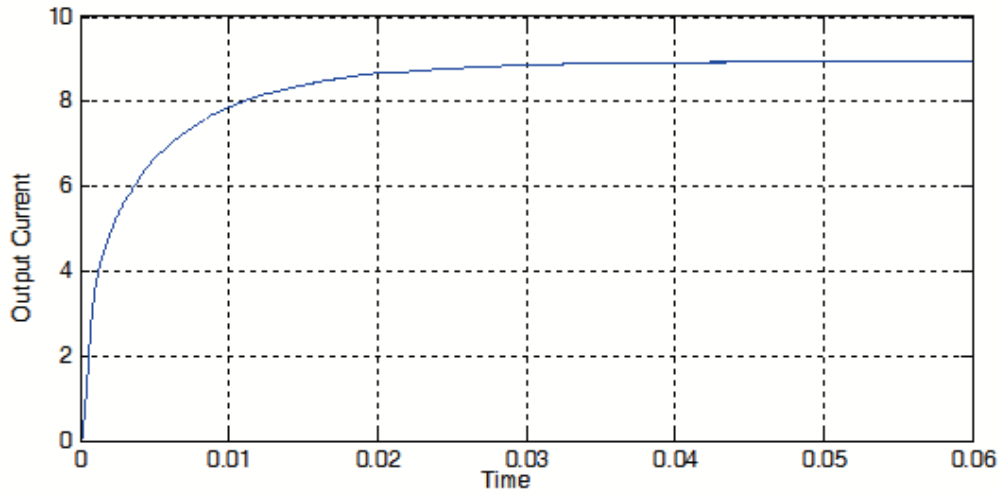
FIGURE 10. Output current to six phase IDDB

of the adopted simplifications, the full-system model has been considered variations in the components.

Now coming to six phase IDDB, the current flowing to the inductance of the six phases is shown in Figure 11. From the above it is clearly observed the current in each inductance is varying from 10 A to 20 A respectively. Output current is shown Figure 10. In this it is observed the output current value is maintained constant. From Figure 8 it is clearly observed that the sliding surface also came to constant.

As the number of phases is increasing with the same input voltage. The input current value reduced but the output current value increased nearly 6.5 A to 9 A, respectively. The output voltage also increased nearly 400 V to 500 V and it is shown in Figure 12. With this it is observed that increasing the number of phases in IDDB with same input then the power handling capability of the converter is increasing.

5. **Conclusions.** This paper has briefed the modelling of the general N-phase IDDB and small signal analysis has been carried out. The sliding mode control design for this converter is illustrated for two-phase as well as six-phase IDDB. It is evident from the results that as the number of phases increases, the power handling capability of the converter is found to be increasing. Hence, the converter can be upgraded with more
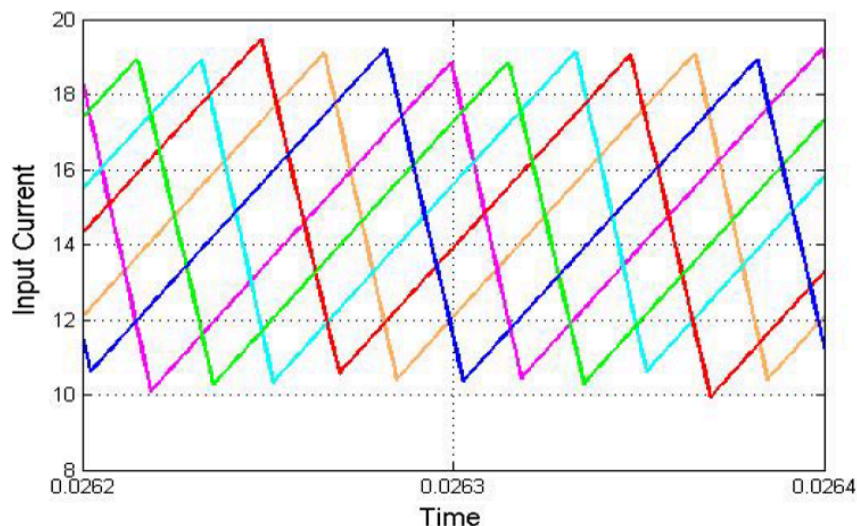
FIGURE 11. (color online) Input current to six phase IDDB
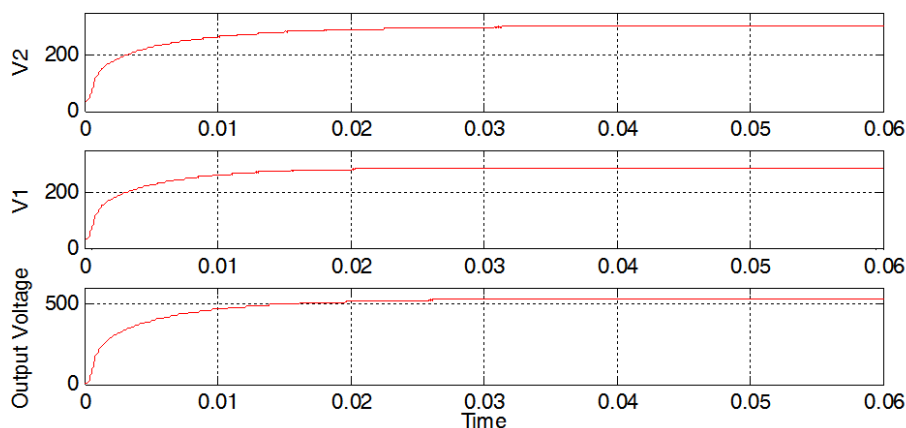
FIGURE 12. Output voltage of six phase IDDB

number of phases as per the load requirements. The symmetry of the converter and the control action were utilized in order to reduce the complexity of the model. Simulation results in MATLAB/Simulink were provided in support of the theoretical analysis. In future, the output of DC-DC boost converter is given to inverter to drive a PMSM with suitable controller.

REFERENCES

[1] H. El Fadil, F. Giri, S. M. Ieee, J. M. Guerrero and S. Member, Modeling and nonlinear control of FC/supercapacitor hybrid energy storage system for electric vehicles, *IEEE Trans. Vehicular Technology*, vol.63, no.7, pp.3011-3018, 2014.

[2] P. Thounthong, P. Sethakul and B. Davat, Modified 4-phase interleaved fuel cell converter for high-power high-voltage applications, *Proc. of IEEE Int. Conf. Ind. Technol.*, pp.1-6, 2009.

[3] F. S. Garcia, J. A. Pomilio and G. Spiazzi, Modeling and control design of the six-phase interleaved double dual boost, *Proc. of the 9th IEEE/IAS Int. Conf. Ind. Appl.*, pp.1-6, 2010.

[4] S. Choi, V. G. Agelidis, J. Yang, D. Coutellier and P. Marabeas, Analysis, design and experimental results of a floating-output interleaved-input boost-derived DC-DC high-gain ransformer-less converter, *IET Power Electron.*, vol.4, no.1, pp.168-180, 2011.

[5] Y. Jang and M. M. Jovanovi'c, Interleaved boost converter with intrinsic voltage-doubler characteristic for universal-line PFC front end, *IEEE Trans. Power Electron.*, vol.22, no.4, pp.1394-1401, 2007.

[6] H. Nomura, K. Fujiwara and M. Yoshida, A new DC-DC converter circuit with larger step-up/down ratio, *Proc. of IEEE Power Electron. Spec. Conf.*, pp.1-7, 2006.

[7] A. Shahin, M. Hinaje, J.-P. Martin, S. Pierfederici, S. Rael and B.Davat, High voltage ratio DC-DC converter for fuel-cell applications, *IEEE Trans. Ind. Electron.*, vol.57, no.12, pp.3944-3955, 2010.

[8] L. S. Yang, T. J. Liang, H. C. Lee and J. F. Chen, Novel high step-up DC-DC converter with coupled-inductor and voltage-doubler circuits, *IEEE Trans. Ind. Electron.*, vol.58, no.9, pp.4196-4206, 2011.

[9] A. Kanchanaharuthai and E. Mujjalinvimut, An improved backstepping sliding mode control for power systems with superconducting magnetic energy storage system, *International Journal of Innovative Computing, Information and Control*, vol.15, no.3, pp.891-904, 2019.

[10] R. Rubpongse, F. Asadi, W. Do and K. Eguchi, Experiment of a high voltage gain switched capacitor DC-DC converter based on a cross-connected fibonacci-type converter, *ICIC Express Letters*, vol.13, no.5, pp.393-400, 2019.